SANDIA REPORT

SAND2006-5419
Unlimited Release
Printed September 2006

Accelerated Aging of Solid Lubricants for the W76-1 TSL: Effects of Polymer Outgassing

Michael T. Dugger, Elizabeth M. Huffman and William O. Wallace

Prepared by
Sandia National Laboratories
Albuquerque, New Mexico 87185 and Livermore, California 94550

Sandia is a multiprogram laboratory operated by Sandia Corporation,
a Lockheed Martin Company, for the United States Department of Energy's
National Nuclear Security Administration under Contract DE-AC04-94AL85000.

Issued by Sandia National Laboratories, operated for the United States Department of Energy by Sandia Corporation.

Available to DOE and DOE contractors from
U.S. Department of Energy
Office of Scientific and Technical Information
P.O. Box 62
Oak Ridge, TN 37831

Telephone: (865) 576-8401
Facsimile: (865) 576-5728
E-Mail: reports@adonis.osti.gov
Online ordering: http://www.osti.gov/bridge

Available to the public from
U.S. Department of Commerce
National Technical Information Service
5285 Port Royal Rd.
Springfield, VA 22161

Telephone: (800) 553-6847
Facsimile: (703) 605-6900
E-Mail: orders@ntis.fedworld.gov
Online order: http://www.ntis.gov/help/ordermethods.asp?loc=7-4-0#online

SAND2006-5419
Unlimited Release
Printed September 2006

Accelerated Aging of Solid Lubricants for the W76-1 TSL: Effects of Polymer Outgassing

Michael T. Dugger, Elizabeth M. Huffman and William O. Wallace

Sandia National Laboratories
P.O. Box 5800
Albuquerque, New Mexico 87185-0889

Abstract

The behavior of MoS_2 lubricants intended for the W76-1 TSL was evaluated after 17 and 82 thermal cycles, each lasting seven days and including a low temperature of -35°C and a high temperature of 93°C, in a sealed container containing organic materials. The MoS_2 was applied by tumbling with MoS_2 powder and steel pins (harperized), or by spraying with a resin binder (AS Mix). Surface composition measurements indicated an uptake of carbon and silicon on the lubricant surfaces after aging. Oxidation of the MoS_2 on harperized coupons, where enough MoS_2 was present at the surface to result in significant Mo and S concentrations, was found to be minimal for the thermal cycles in an atmosphere of primarily nitrogen. Bare steel surfaces showed a reduction in friction for exposed coupons compared to control coupons stored in nitrogen, at least for the initial cycles of sliding until the adsorbed contaminants were worn away. Lubricated surfaces showed no more than a ten percent increase in steady-state friction coefficient after exposure. Initial coefficient of friction was up to 250 percent higher than steady-state for AS Mix films on H950 coupons after 82 thermal cycles. However, the friction coefficient exhibited by lubricated coupons was never greater than 0.25, and more often less than 0.15, even after the accelerated aging exposures.

Acknowledgments

The authors are grateful for the help of Jason Brown and Steve Thornberg (both 1825) in analyzing the residual gases present in aged canisters containing lubricated samples, and to Amy Rice (1523), Alan Mortensen (5332) and Benjamin Garnas (2613) for preparing lubricated samples and conducting the accelerated aging thermal exposures. Financial support was provided by the W76 and W80 Life Extension Programs, and is gratefully acknowledged.

Contents

1. Introduction 9
2. Experimental Procedures 10
2.1 Lubricant Aging Samples 10
2.2 Aging Canisters 11
2.3 Thermal Cycles 12
2.4 Surface Chemical Analysis 12
2.5 Friction Coefficient Measurement 13
3. Results and Discussion 15
3.1 Residual Gas Analysis 15
3.2 Surface Composition 15
3.2 Impact of Aging on Friction Behavior 19
4. Conclusions 24
References 24
Appendix A. Details on PH 13-8 Mo Material 25

List of Figures

Page

Figure 1. Coupons used to evaluate changes in friction due to accelerated aging, from left to right, are unlubricated, AS Mix lubricated, and MoS_2 harperized 10

Figure 2. Temperature-time profile for one thermal cycle. Numbers next to the temperature profile indicate the time in hours of the ramp or thermal soak 12

Figure 3. Tribology test equipment used for friction measurements. A controlled-envioronment glovebox (a) houses the rotary pin-on-disk tester (b). 14

Figure 4. Elemental composition for the unlubricated coupons of 13-8 Mo stainless steel, H950 and H1150 heat treatments, in the control and aged conditions 15

Figure 5. Elemental composition for the AS Mix lubricated coupons in H950 and H1150 heat treatments, in the control and aged conditions 16

Figure 6. Elemental composition for the MoS_2 harperized coupons in H950 and H1150 heat treatments, in the control and aged conditions 16

Figure 7. S/Mo atomic concentration ratios for the MoS_2 harperized coupons in H950 and H1150 heat treatments, for both control and aged conditions 17

Figure 8. Mo 3p XPS spectral region used to determine the ratio of Mo oxide to sulfide for MoS_2 harperized on stainless steel. Examples shown are for sample 79, aged for 82 thermal cycles (a), and the same film on 15-5 PH stainless steel (b) from another study, baked at 250°C for 4 hours in air with 15950 ppm H_2O (50% RH)..... 18

Figure 9. S/Mo atomic concentration ratios for the MoS_2 harperized coupons in H950 and H1150 heat treatments, for both control and aged conditions 19

Figure 10. Friction coefficient versus number of sliding cycles for the H950 coupons without lubricant (a), with AS Mix (b), and MoS_2 harperized (c) coatings, as a function of exposure conditions. Each curve is the average of four individual measurements..... 20

Figure 11. Friction coefficient versus number of sliding cycles for the H1150 coupons without lubricant (a), with AS Mix (b), and MoS_2 harperized (c) coatings, as a function of exposure conditions. Each curve is the average of four individual measurements..... 21

Figure 12. Optical micrographs of disk wear tracks on unlubricated coupons (a-b), AS Mix lubricated coupons (c-d), and MoS_2 harperized coupons (e-f)..... 23

List of Tables

Page

Table I. Coupon Numbers and Conditions 11

Table A-I. Composition of 13-8 Mo Stainless Steel..... 25

Table A-II. Typical PH 13-8 Mo Mechanical Properties 25

Nomenclature

AS Mix	Allied Signal Mix, MoS_2 + graphite particles in an epoxy matrix
FM&T	Federal Manufacturing and Technologies (Honeywell)
PH	Precipitation Hardened (stainless steel)
PMDI	Polymeric Methylene DiIsocyanate (foam)
RGA	Residual Gas Analysis
RH	Relative Humidity
TSL	Trajectory Safing Stronglink
XPS	X-ray Photoelectron Spectroscopy
SNL	Sandia National Laboratories

1. Introduction

Solid lubricants are used in many weapon components, including stronglinks and environment sensing devices, in order to control friction during operation and prevent seizure during long term storage and transportation of the components. Many such components are hermetically sealed with an inert internal atmosphere to minimize oxidation and corrosion. MoS_2-based solid lubricants perform well in environments lacking oxygen and water vapor, and are a frequent choice of design engineers for the surfaces of parts that experience impact, rolling and sliding.

The most common degradation mechanism for MoS_2-based solid lubricants exposed to normal environments in weapon mechanisms is oxidation. Oxygen or water vapor may be present in the internal atmosphere due to outgassing of other materials inside the component, principally organic materials, or due to ingress through a leak. There may even be small amounts of water sealed inside the device, since the last monolayer of water adsorbed on solid surfaces can be very difficult to remove. Over decades of aging in non-leaking devices, outgassing or interactions with species inside the sealed volume is the primary source of any reactions affecting the frictional behavior of solid lubricants. One method of assessing the effects of outgassing or material interactions on the performance of solid lubricants is through accelerated aging studies. In this case, samples of the solid lubricant material are placed in a sealed volume with other materials present in the component, and then subjected to thermal soaks or cycles intended to represent a longer term aging environment.

The analyses performed to evaluate the effects of aging on solid lubricants for the W76-1 TSL in this report represent the conclusions of a two-part aging assessment. In the first part, whose results were previously documented [1], lubricated coupons were aged for 17 thermal cycles, each lasting seven days, in a sealed container with polyurethane foam and silicone gasket material. Slight increases in adsorbed carbon and silicon, and less than 10 percent increase in friction coefficient, μ, of the solid lubricant coatings were observed for that exposure. In the second part of the study, the same temperature profile was continued for 82 cycles lasting a total of 598 days. A second set of lubricated coupons was included in this canister, which contained slightly different quantities of the same organic materials as the first aging exposure. The entire set of results from both aging intervals, and a discussion, are presented in this report for completeness.

2. Experimental Procedures

2.1 Lubricant Aging Samples

Substrate materials selected for the lubricant aging studies consisted of 13-8 Mo stainless steel coupons, 25.4 mm (1 inch) in diameter and 1 mm (0.039 inch) thick. This steel is precipitation hardenable (PH) through heat treatment. The coupons were prepared in two different heat treatments, H950 and H1150, to simulate the materials and heat treatments used in parts for the W76-1 TSL. Coupon composition and heat treatment parameters are described in Appendix A.

Coupons were either bare or lubricated with MoS_2 using two different processes. The bare coupons were tested in the as-machined condition, and cleaned to remove residual contamination. One set of lubricated coupons was produced using sprayed, resin-bonded MoS_2. In this process, referred to as "AS Mix," the coupon is first blasted with an aqueous slurry of Al_2O_3 particles to roughen the surface and improve coating adhesion. The coupon is then cleaned, and a mixture of MoS_2 powder and a liquid resin is sprayed onto the metal surface. These processes are discussed in detail in specification SS393040. The lubricant is then cured and burnished. Burnishing consists of rubbing the surface with a fiber brush to remove poorly-adhered particles of the lubricant.

The other set of lubricated coupons was produced using harperization, where the coupons were tumbled with MoS_2 powder in a drum along with steel pins. The MoS_2 particles are crushed during impacts between the parts and the steel pins, and result in a very thin "transfer film" of MoS_2 on the steel surface. The layer is referred to as a transfer film since MoS_2 is transferred to the surface of interest during the process of crushing and shearing of the MoS_2 particles. This process is described in more detail in specification SS1A5910. The lubricants were applied to the coupons at Honeywell FM&T in both cases. A photograph showing the surface finish typical for each of the treatments is shown in Figure 1.

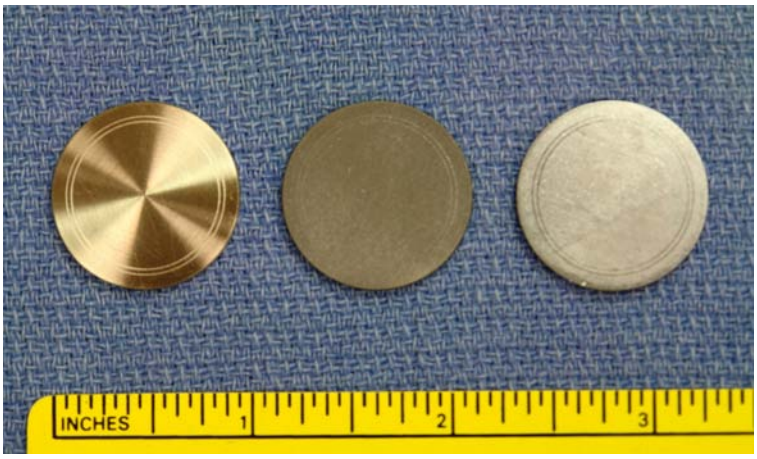

Figure 1. Coupons used to evaluate changes in friction due to accelerated aging, from left to right, are unlubricated, AS Mix lubricated, and MoS_2 harperized. The circular marks near the outer diameter are wear tracks created during testing.

Table I shows the coupon numbers that were tested, and corresponding heat treatment, aging condition, and surface treatment.

Table I. Coupon Numbers and Conditions

Heat Treatment	Thermal Cycles	Coupon Number		
		Unlubricated	AS Mix	MoS_2 Harperized
H950	None-Control	87	80	77
H950	17 Cycles	86	83	76
H950	82 Cycles	85, 88	81, 84	78, 79
H1150	None-Control	63	58	50
H1150	17 Cycles	62	59	53
H1150	82 Cycles	61, 64	57, 60	52, 54

After manufacture and coating of the coupons with solid lubricant, a set of "control" samples including unlubricated, AS Mix, and MoS_2 harperize-coated coupons were stored at 22±3°C in a nitrogen-purged desiccator. Another group of coupons were designated for sealing in the 17 cycle aging canister, and a third set in the 82 cycle aging canister. The control samples were analyzed at the same time as the 17 cycle aging samples, when they were removed from their canister.

2.2 Aging Canisters

The bare and lubricated coupons were placed in cylindrical stainless steel chambers having inner diameter of approximately 15 cm and length of about 20 cm. The chambers were backfilled with a starting gas mixture of 90% N_2 and 10% He. The chambers contained the following materials:

17 Cycle Canister:

A. PMDI Polyurethane foam (per materials specification 9927115 using materials per 2170427 and 2170421) with a total volume of 16.39 cm^3 (1 in^3), having approximate density of 0.224 to 0.240 g/cm^3 (14-15 lbs/ft^3).
B. Four sponge gasket parts per AY1A3628 (made of Chorlastic R-10470 silicone medium closed cell sponge rubber from CHR Industries), each part having volume of 0.213 cm^3 (0.013 in^3) for a total volume of 0.852 cm^3 (0.052 in^3). The density of this material is approximately 0.471 g/cm^3 (0.017 lb/in^3).
C. Stainless steel coupons for lubricant aging evaluation, as noted in Table I.

82 Cycle Canister:

A. PMDI Polyurethane foam (per materials specification 9927115 using materials per 2170427 and 2170421) with a total volume of 32.78 cm^3 (2 in^3), having approximate density of 0.224 to 0.240 g/cm^3 (14-15 lbs/ft^3).
B. Eight sponge gasket parts per AY1A3628 (made of Chorlastic R-10470 silicone medium closed cell sponge rubber from CHR Industries), each part having volume of 0.213 cm^3 (0.013 in^3) for a total volume of 1.704 cm^3 (0.104 in^3). The density of this material is approximately 0.471 g/cm^3 (0.017 lb/in^3).

C. Quartz crystal (unspecified dimensions).
D. Stainless steel coupons for lubricant aging evaluation, as noted in Table I.

2.3 Thermal Cycles

The chambers were sealed and aged using the temperature profile shown in Figure 2. The temperature cycle shown takes 7 days, and was repeated approximately 17 times for the first canister and 82 times for the second canister. At the conclusion of the thermal cycling experiments, the internal atmospheres of the canisters were sampled using RGA, and the stainless steel coupons were removed for surface analysis and friction measurements.

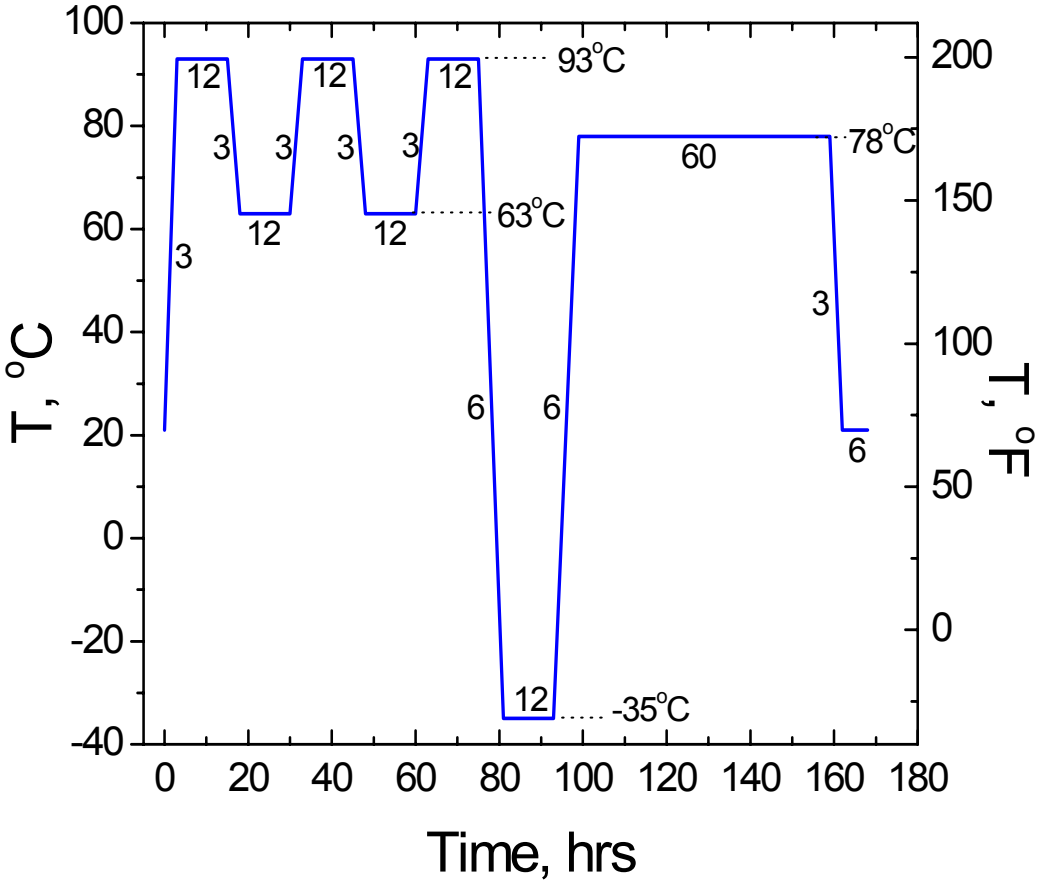

Figure 2. Temperature-time profile for one thermal cycle. Numbers next to the temperature profile indicate the time in hours of the ramp or thermal soak.

2.4 Surface Chemical Analysis

The chemical composition of the coupons was measured using x-ray photoelectron spectroscopy (XPS). Monochromatic Al Kα radiation was used in a Kratos Axis Ultra system with a delay-line detector. The atomic concentration of major constituents was determined using standard sensitivity factors for the elements. In addition, for the 82 cycle (second) canister, the oxidation of the MoS_2 on the lubricated surfaces was

evaluated by determining the amount of oxide and sulfide present as revealed in the high resolution scans of the S 2p and Mo 3p spectral regions.

2.5 Friction Coefficient Measurement

Friction tests were performed using a 440C stainless steel bearing ball 1.59 mm (0.0625 inch) in diameter as the mating surface. A pin-on-disk friction tester produced a circular wear track of approximately 20 mm diameter. Sliding experiments were conducted at a load of 14.3 gf (peak Hertzian contact pressure of 812 MPa), an average interfacial velocity of 42 mm/s, and for 1000 revolutions of the disk (cycles). The steel ball was held in a ball holder at the end of a horizontal beam. The beam was outfitted with strain gauges to permit measurement of the friction forces, and the normal load was provided by a dead weight. The disk was held in the jaws of a stage that rotated on a motor spindle. These contact conditions produced a circular apparent contact area of 18 μm diameter (based on static Hertzian contact mechanics), and maximum shear stress located about 4 μm below the surface. Testing in this way concentrated the deformation near the surface and accentuated any changes in friction behavior due to lubricant oxidation or contaminant adsorption. The experiments were conducted in a glovebox purged with nitrogen, having oxygen concentration (Delta F oxygen analyzer, platinum series) less than 10 ppmv, and water vapor concentration (General Eastern M4 chilled mirror hygrometer) less than 200 ppmv. Photographs of the test equipment are shown in Figure 3.

Four friction measurements were made for each condition of substrate heat treatment, lubricant, and aging condition. This typically resulted in two friction traces on each sample. The friction traces were averaged to create a single trace of friction coefficient, μ, as a function of sliding cycles that represents the typical behavior of the lubricant for the specified aging conditions.

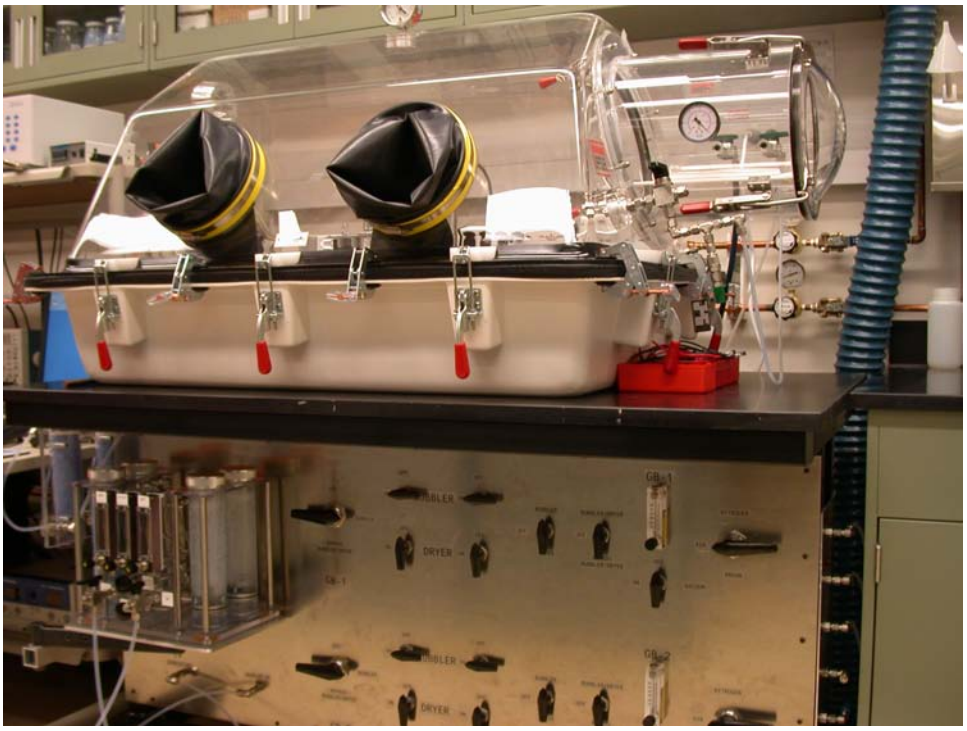

(a)

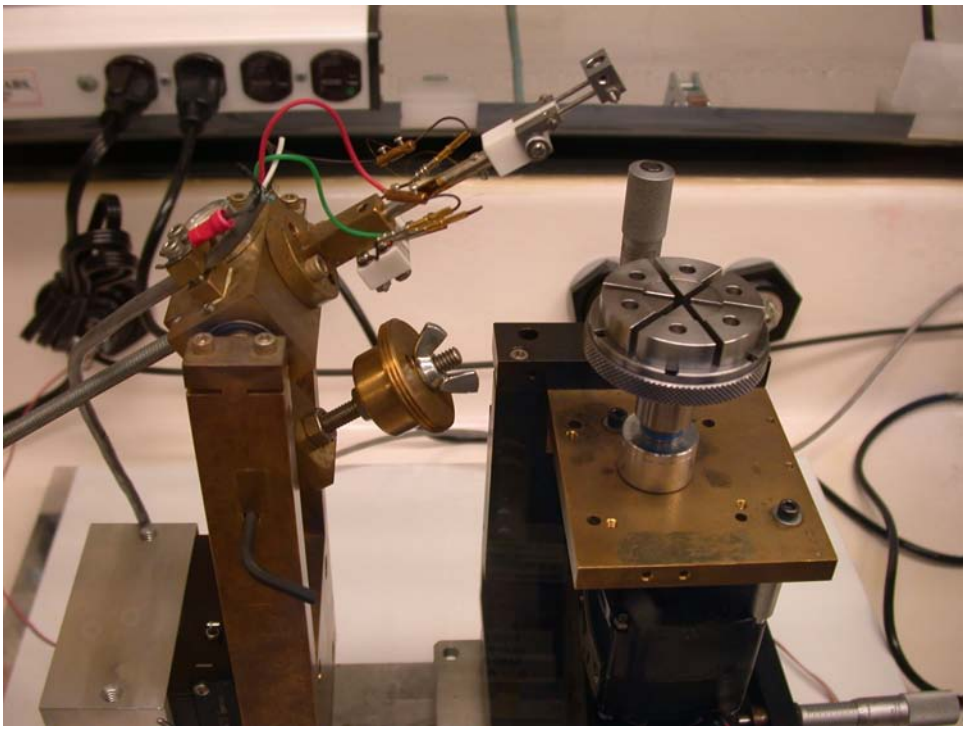

(b)

Figure 3. Tribology test equipment used for friction measurements. A controlled-envioronment glovebox (a) houses the rotary pin-on-disk tester (b).

3. Results and Discussion

3.1 Residual Gas Analysis

The final gas composition within the 17 cycle canister was measured to be 91 vol.% N_2, 8% He, and less than 1% each of CO_2, O_2 and H_2.

For the 82 cycle canister, mass spectrometry and RGA of the headspace in the canister revealed an atmosphere comprised almost entirely of nitrogen. Additionally, there was < 0.1% each of CO_2 and Ar present, along with trace amounts of CO, H, and He. No other constituents were detected. Base on this analysis, there may have been a small leak in the second canister that permitted the He leak detection gas to escape. Since no oxygen was detected, this is not expected to influence the aging results of the lubricants in this canister.

3.2 Surface Composition

The surface elemental composition determined by XPS for all samples is shown in Figures 4-6. Elements not listed in the figures were not detected. Figure 4 shows the

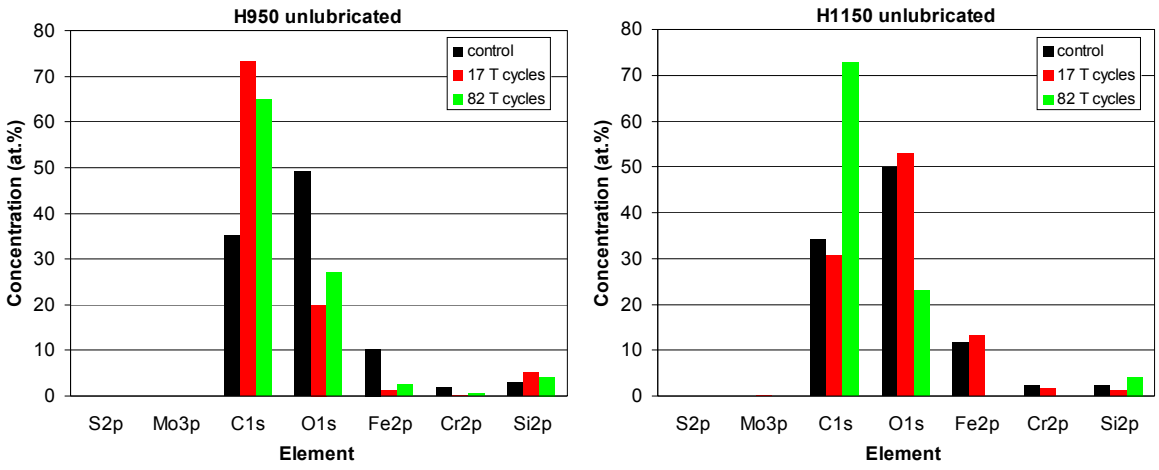

Figure 4. Elemental composition for the unlubricated coupons of 13-8 Mo stainless steel, H950 and H1150 heat treatments, in the control and aged conditions.

composition of the unlubricated stainless steel surfaces in the control, 17 cycle and 82 cycle aging exposure conditions. These coupons had undetectable amounts of S and Mo, consistent with the lack of lubrication on these samples. Carbon and oxygen are prevalent as is typical during surface analysis (sensitive to only the top ~5 nm of the surface) of samples exposed to the atmosphere. Iron and chromium, the largest metallic constituents of the alloy, are detected. Silicon is also detectable in the control as well as aged samples. The aged samples show a slight increase in Si concentration, and a significant uptake of carbon, particularly for the samples aged for 82 thermal cycles. This change is consistent with the metallic surface adsorbing carbonaceous species outgassed from the polymeric materials in the aging canisters, particularly from the silicone foam gasket material.

Figure 5 shows the surface composition data for the AS Mix lubricated coupons. In this case, the constituents of the lubricant layer are detectable, but only at the level of a

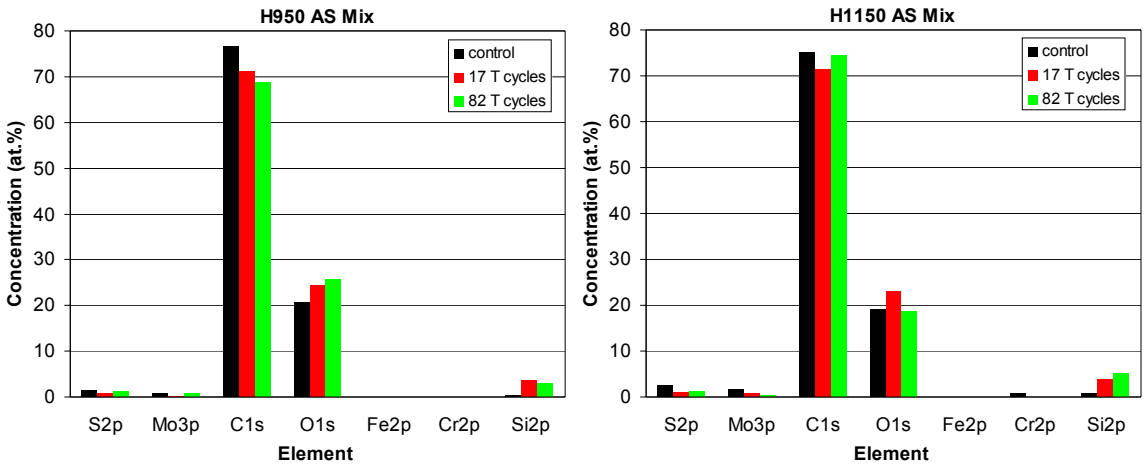

Figure 5. Elemental composition for the AS Mix lubricated coupons in H950 and H1150 heat treatments, in the control and aged conditions.

few atomic percent. Carbon dominates these spectra, due both to atmospheric contamination as discussed above, and to the epoxy resin used as a binder for the MoS_2 particles. Iron and chromium are barely detected, if at all, but there exists a significant silicon peak, particularly in the aged samples. This would suggest strong adsorption of outgassing products from the silicone foam rubber samples.

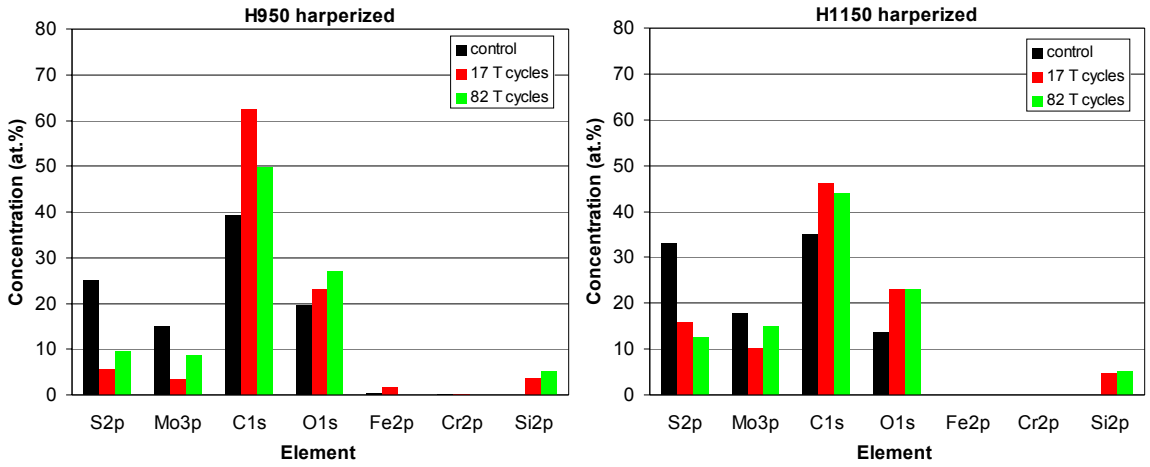

Figure 6. Elemental composition for the MoS_2 harperized coupons in H950 and H1150 heat treatments, in the control and aged conditions.

Figure 6 shows the surface composition data for the MoS_2 harperized coupons. In this case, the S and Mo are present in larger quantities than for the AS Mix lubricated coupons, since there is no binder present to cover the lubricating particles. The control coupons show these elements present in roughly a 2:1 ratio, as would be expected from

the atomic ratios in the compound. Carbon and oxygen are present due to adsorbates and oxidized substrate metals, although the latter are a minor contributor to the total oxygen signal since small quantities of Fe and Cr are detected only in the H950 samples. The lack of these substrate species on the H1150 samples may suggest variations in the harperized layer thickness, and masking of the substrate by Mo and S on these coupons. All of these coupons show increased Si concentration after aging, once again suggesting adsorption of outgassing products from the silicone foam in the canisters.

In summary, the atomic concentration data suggests that the coupons adsorb carbonaceous outgassing products from the polymeric materials inside the aging canisters, although this contaminant adsorption is not sufficient to completely mask the S and Mo peaks on the lubricated surfaces. This suggests that the contaminant layer is less than about 5 nm thick. The increase in silicon concentration suggests that the silicone foam in the canisters contributes at least a portion of this outgassing material.

Changes in the atomic concentrations of sulfur and molybdenum present in the lubricant coatings provide some information on the degree of lubricant degradation as a function of aging exposure. The unlubricated coupons exhibited no detectable S and Mo, and the concentrations of these elements present on the AS Mix lubricated samples was very low due to the presence of the binder phase, which masked the signal from the MoS_2 particles. However, the S and Mo concentration in the harperized samples is sufficient to provide a reliable determination of the degree of lubricant degradation with aging. Specifically, the S/Mo atomic concentration ratio will reveal loss of sulfur with age, since the sulfate species formed by oxidation of the MoS_2 are volatile, and cause a loss of sulfur from the surface. The S/Mo ratios for the harperized coupons in this work are shown in Figure 7. The figure shows that for both types of substrates, the 82 thermal

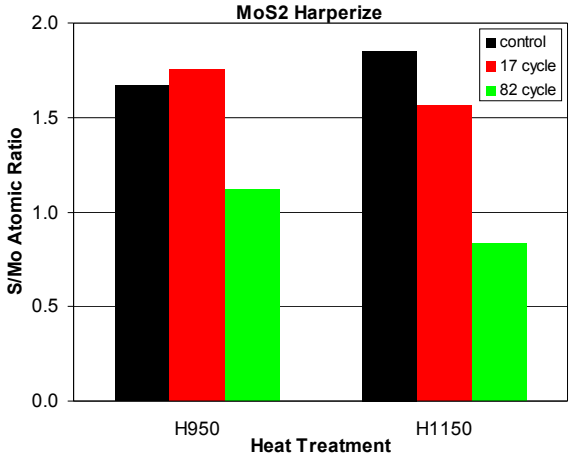

Figure 7. S/Mo atomic concentration ratios for the MoS_2 harperized coupons in H950 and H1150 heat treatments, for both control and aged conditions.

cycle exposure results in a significant loss of sulfur compared to the control and the 17 thermal cycle exposure. The MoS_2 particles should exhibit a S/Mo ratio of 2 for the non-degraded, stoichiometric compound. The control coupons exhibit ratios between 1.7 and

1.9, which may reflect inaccuracies in the sensitivity factors for detection of these elements in the XPS, or some real slight loss of sulfur from the surface of the control samples during exposure to air. There is only moderate change from the control values for the 17 cycle exposure. However, S/Mo ratios for the 82 cycle exposure indicate a significant loss of sulfur from the surface.

In addition to the atomic concentration data discussed above, high resolution XPS spectra were acquired for the 82 cycle aging coupons to quantify the degree of lubricant degradation that may have occurred during thermal cycles. This process involves acquiring XPS data around the S 2p and Mo 3p regions, fitting the observed spectrum with peaks corresponding to the binding energies for the oxide and sulfide (in the case of Mo), or sulfide and sulfate (in the case of S 2p), and then deconvoluting the observed spectrum into contributions from the oxide and sulfide species. This process is illustrated in Figure 8 for the Mo 3p spectral region, acquired from coupon 79, and the same film on 15-5 PH stainless steel and baked in humid air analyzed in a related project. The increase in the peaks for the Mo oxide compared to the sulfide is evident in (b). The area of the

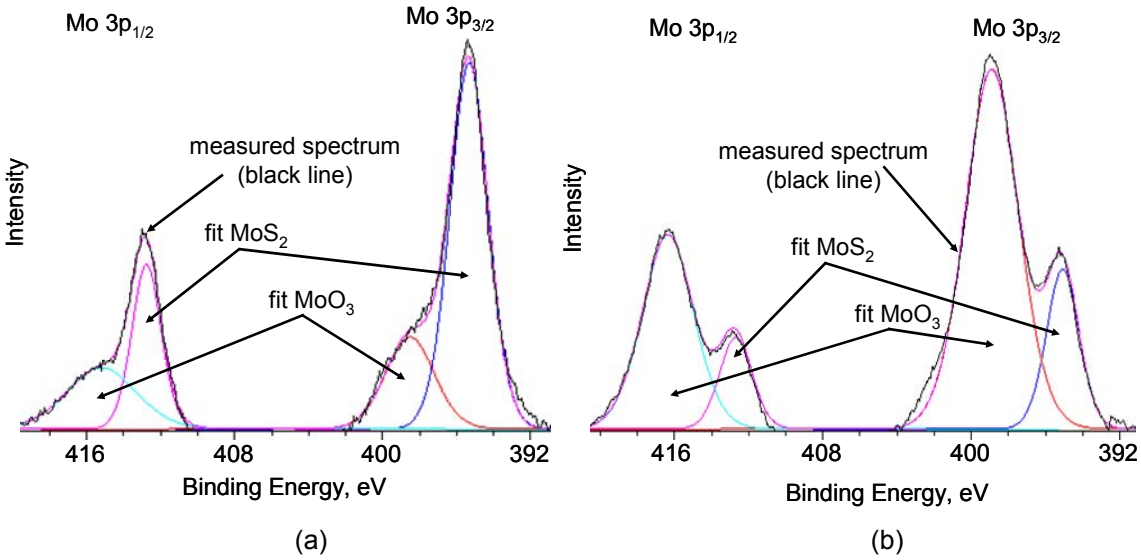

Figure 8. Mo 3p XPS spectral region used to determine the ratio of Mo oxide to sulfide for MoS_2 harperized on stainless steel. Examples shown are for sample 79, aged for 82 thermal cycles (a), and the same film on 15-5 PH stainless steel (b) from another study, baked at 250°C for 4 hours in air with 15950 ppm H_2O (50% RH).

constituent peaks allows the concentration of the oxide (MoO_3) and sulfide (MoS_2) to be determined separately. Since the MoO_3 is not volatile, it provides a more reliable measurement of the degree of oxidation of the lubricant particles than does analysis of the sulfur peaks.

Using the process described above, the Mo oxide to sulfide ratio was determined for the MoS_2 harperized samples aged in this study, and compared to that for the same type of MoS_2 film on 15-5 PH stainless steel substrates aged as part of a separate study. In that study, MoS_2 harperized coatings were deposited on 15-5 PH stainless steel and

subjected to a variety of time, temperature, and environment conditions to determine the effects of component purge and backfill processes on the surface chemistry of the lubricant, as well as the effects of heating in a humid environment for comparison. The results are shown in Figure 9. The H950 and H1150 coupons aged for 82 thermal cycles in this study exhibit a slightly higher oxide to sulfide ratio than the 15-5 coupon baked in low vacuum (125°C for 4 hours at 10^{-5} Torr), but less than half the Mo is oxidized over the depth analyzed by XPS. In contrast, the 15-5 PH sample subjected to the "humid bake" (250°C for 4 hours in air with 15590 ppm H_2O) exhibits significant oxidation of the MoS_2 to form MoO_3. In short, the thermal cycles used to emulate accelerated aging

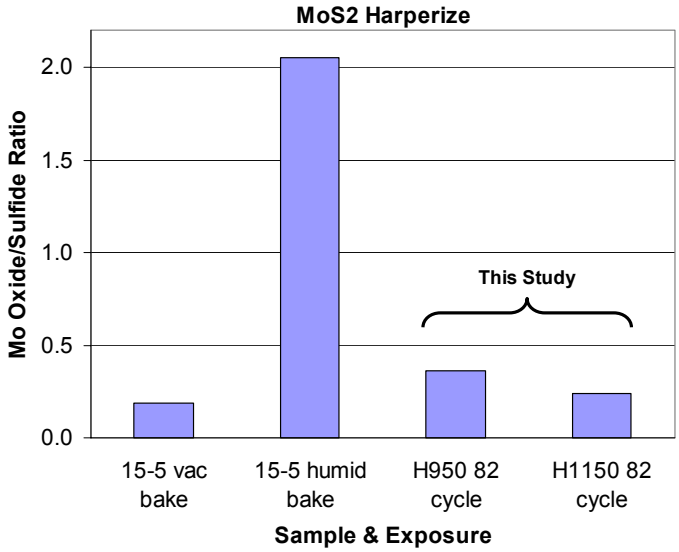

Figure 9. S/Mo atomic concentration ratios for the MoS_2 harperized coupons in H950 and H1150 heat treatments, for both control and aged conditions.

of the lubricated coupons in this study were not severe in terms of lubricant oxidation. Of course this is due in large part to the fact the canisters were filled with inert gas prior to the thermal exposures. The main change to the lubricated surfaces due to the exposures is the adsorption of contaminants due to the outgassing of polymeric materials inside the sealed volumes. The effects of this change in surface composition on tribological behavior will be examined in the next section.

3.2 Impact of Aging on Friction Behavior

The friction coefficient as a function of number of sliding contact cycles for the H950 and H1150 coupons is shown in Figures 10 and 11, respectively. Each curve is the average of four measurements, and the changes in friction behavior with aging for 17 and 82 thermal cycles is shown for each surface condition.

The unlubricated, control surfaces (Figures 10a and 11a) exhibit friction coefficient $\mu \sim 0.7$, typical of adhesive wear of the unlubricated steel under these sliding conditions.

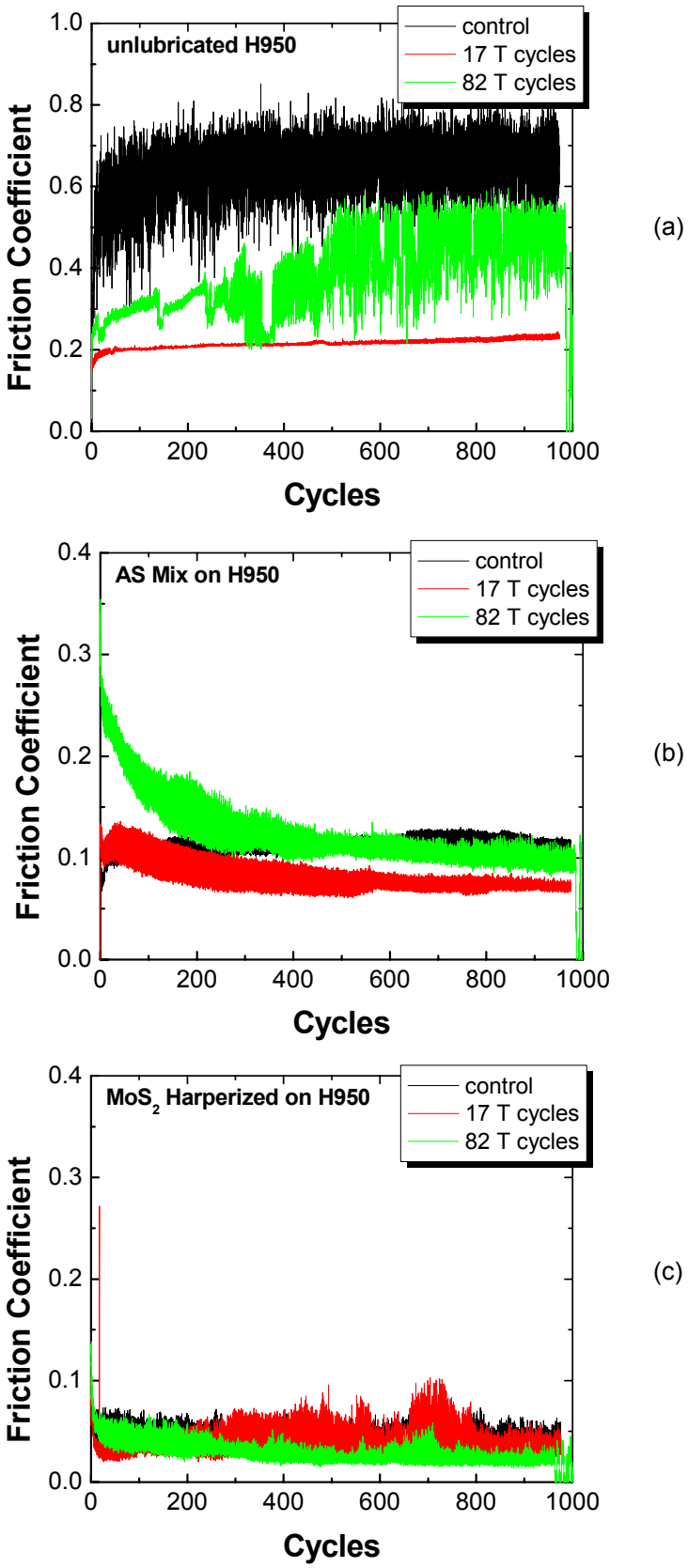

Figure 10. Friction coefficient versus number of sliding cycles for the H950 coupons without lubricant (a), with AS Mix (b), and MoS_2 harperized (c) coatings, as a function of exposure conditions. Each curve is the average of four individual measurements.

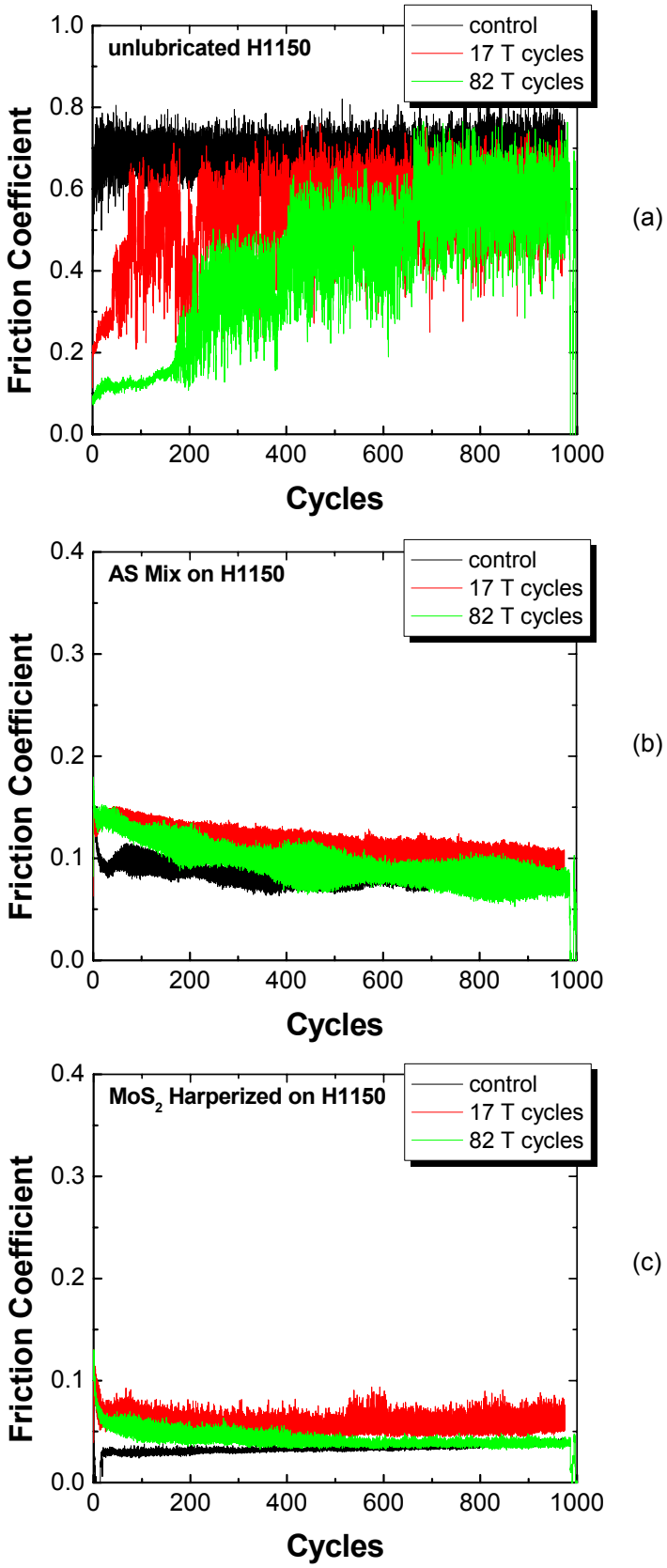

Figure 11. Friction coefficient versus number of sliding cycles for the H1150 coupons without lubricant (a), with AS Mix (b), and MoS_2 harperized (c) coatings, as a function of exposure conditions. Each curve is the average of four individual measurements.

Adhesion between unlubricated steel surfaces results in plastic deformation and high friction characteristic of "stick-slip," that is, micro-welding followed by rupture of the contact, which repeatedly damages the surfaces. Unlubricated surfaces exposed to thermal cycling in the sealed containers exhibit a reduction in friction coefficient, or a delay in the onset of stick-slip. This is due to the presence of adsorbed contaminant layers that prevent metal to metal contact for a short time. These layers are worn through (in the 82 thermal cycle tests), allowing the adhesive interaction between the sliding surfaces to commence.

The surfaces treated with AS Mix MoS_2 (Figures 10b and 11b) exhibit a steady-state friction coefficient of ~0.1, typical for this material in a dry nitrogen atmosphere. The lubricated coupons exposed to accelerated aging exhibit a slightly higher initial friction coefficient, particularly evident in the H950 coupons exposed to 82 thermal cycles which showed an initial friction coefficient of 0.25. However, after about 200 sliding cycles the friction was reduced to levels similar to the control surface, within the variability observed in the measurements. Increases in initial friction coefficient are typically seen in oxidized MoS_2 films since the change in composition that accompanies oxidation results in a change in the shear strength of the material. This layer is worn through after some period of sliding, allowing the unworn MoS_2 to become exposed and form a transfer layer between the two sliding bodies. The surface composition data from XPS showed atomic concentrations of Mo and S (Figure 5) that were too small to make definitive conclusions about the degree of oxidation of the lubricant. However, this data also showed an increase in oxygen and silicon the on thermally-cycled coupons compared to the control surfaces, suggesting that the surfaces adsorbed organic contamination in the form of silicones. This adsorbed material may also be responsible for the initial friction increase, since the environments contained little oxygen.

The friction behavior of surfaces coated with the MoS_2 harperization process is shown in Figures 10c and 11c. This surface treatment results in friction coefficients near 0.05 in a dry nitrogen atmosphere. The friction coefficient observed on the H950 coupons after thermal cycles was unchanged from the control value within the variability observed in the measurements. On the H1150 coupons, the thermally cycled coupons exhibited a slightly higher initial friction, up to about 0.08 compared to the unaged control sample. The surface composition data (Figure 6) shows increases in C, O and Si at the expense of S and Mo, consistent with adsorption of organic contaminants on the lubricant surface. The high resolution XPS spectra for Mo suggest only slight oxidation of the surfaces for the aged coupons, compared to the control surface.

Optical micrographs of the wear tracks on the disks are shown in Figure 12. Figure 12(a) shows two wear tracks on the unlubricated disk, and 12(b) shows the wide track and surface damage associated with high friction, adhesion and stick-slip behavior. Figure 12(c) and (d) show wear tracks on an AS Mix coupon, and illustrate the roughening of the surface caused by Al_2O_3 blasting and resulting discontinuous contact. Figure 12(e) and (f) show wear tracks on a MoS_2 harperized disk. The MoS_2 transfer film is everywhere in Figure 12(e), but thickest in the areas with dark contrast. This material is pulled out of surface valleys and smeared over the wear track during sliding contact.

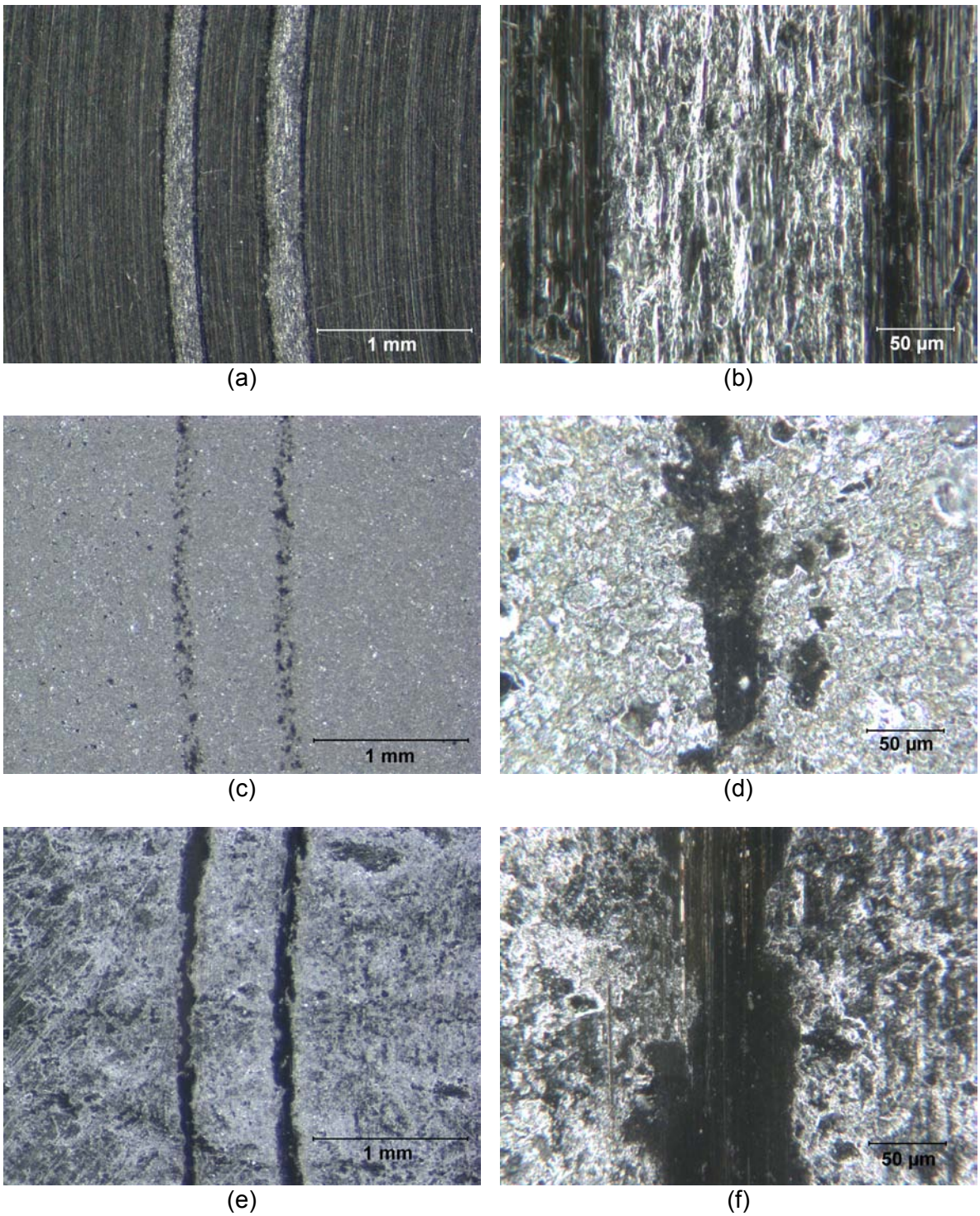

Figure 12. Optical micrographs of disk wear tracks on unlubricated coupon # 61 (a-b), AS Mix lubricated coupon #57 (c-d), and MoS_2 harperized coupon #52 (e-f).

4. Conclusions

Samples of 13-8 stainless steel in hardness conditions H950 and H1150 were lubricated with AS Mix or MoS_2 harperized solid lubricants and subjected to accelerated aging in a sealed container with samples of polymeric materials. The accelerated aging consisted of thermal cycles from -35°C to 93°C. Surface analysis and friction measurements were performed to assess the impact of these accelerated aging environments on the behavior of the solid lubricants for the W76-1 TSL. Accelerated aging results in an increase in carbon, and particularly silicon, concentration on the sample surfaces due to adsorption of outgassing products from the polymeric materials. Measurements of the oxidation state of Mo from the MoS_2 harperized samples, where sufficient Mo concentration permitted detailed analysis of peak shapes, indicated that the lubricant was only slightly more oxidized than the control surfaces that were stored in dry nitrogen after treatment. The major change in surface composition due to aging is therefore the adsorption of a layer of organic contamination. Contamination of lubricated surfaces by outgassing material increased the steady-state friction coefficient by less than 10 percent. The initial friction coefficient was slightly higher than the steady-state value in a few cases, by up to 250 percent in the case of AS Mix on the H950 samples aged for 82 thermal cycles. However, the friction coefficient was less than or equal to 0.25 for all the lubricated samples, and most often less than 0.15.

References

1. Memo from Michael Dugger to Alan Mortensen, subject "Accelerated Aging Effects on the Composition and Friction of Lubricants for the W76-1 TSL," dated 21 April 2005.
2. Armco, Incorporated, One Oxford Centre, 301 Grant Street, Pittsburgh PA 15219-1415.
3. High Temp Metals, Inc., 12910 San Fernando Rd., Sylmar, CA 91342-3601. www.hightempmetals.com/techdata/hitemp13-8MOdata.php

Appendix A. Details on PH 13-8 Mo Material

The composition of the 13-8 stainless steel coupons used as substrates for the solid lubricants in this work are shown in Table A-1, below. PH 13-8 Mo is a registered trademark of Armco, Inc. [2].

Table A-I. Composition of 13-8 Mo Stainless Steel*

Element	Min. wt.%	Max. wt.%
Carbon	--	0.05
Manganese	--	0.10
Silicon	--	0.10
Chromium	12.25	13.25
Nickel	7.50	8.50
Nitrogen	--	0.01
Sulfur	--	0.008
Phosphorus	--	0.01
Aluminum	0.90	1.35
Molybdenum	2.00	2.50

*From reference [3]

PH 13-8 Mo stainless is hardened by starting with the solution-treated material (Condition A), and then holding at a specific temperature and time to achieve the desired hardness. The heat treatments relevant to the W76-1 TSL are H950 and H1150.

Condition A
Heat to 1700+/-15°F (dependent on section size) and hold for at least one hour, then cool to below 60°F so that the material is completely transformed to martensite. Sections under 36 square inches are typically water-quenched.

H950
Heat solution-treated material to 950+/-10°F for 4 hours, then air cool.

H1150
Heat solution-treated material to 1150+/-10°F for 4 hours, then air cool.

Table A-II. Typical PH 13-8 Mo Mechanical Properties*

Heat Treatment	Modulus of Elasticity, GPa	0.2% Yield Strength, MPa	Ultimate Strength, MPa	% Elongation	Hardness, Rockwell C	Charpy Impact Strength, Joule
H950	195	1449	1551	12	47	27
H1150	195	724	1000	20	33	103

*From reference [3]

Distribution:

1	MS0319	J.G. Dabling	2613
1	MS0319	T.N. Hinnerichs	2613
1	MS0319	A.M. Ison	2613
1	MS0319	K.A. Klody	2613
1	MS0319	J.T. McLaughlin	2613
1	MS0319	S.D. Summers	2613
1	MS0501	J. Brown	5332
1	MS0501	A. Mortensen	5332
1	MS0886	W.O. Wallace	1822
1	MS0889	M.T. Dugger	1824
1	MS0889	E.M. Huffman	1824
1	MS0889	S.V. Prasad	1824
2	MS9018	Central Technical Files	8944
2	MS0899	Technical Library	4536